

Article

Novel Approach for the Approximation of Vitamin D₃ Pharmacokinetics from In Vivo Absorption Studies

Grzegorz Żurek ¹, Magdalena Przybyło ^{2,3}, Wojciech Witkiewicz ⁴ and Marek Langner ^{2,3,*}

¹ Faculty of Pure and Applied Mathematics, Wrocław University of Science and Technology, 51-270 Wrocław, Poland

² Lipid Systems sp. z o.o., 54-613 Wrocław, Poland

³ Department of Biomedical Engineering, Faculty of Fundamental Problems of Technology, Wrocław University of Science and Technology, 51-270 Wrocław, Poland

⁴ Research and Development Centre, Specialized Hospital in Wrocław, 51-124 Wrocław, Poland

* Correspondence: marek.langner@lipid-systems.pl

Abstract: The changing environment and modified lifestyles have meant that many vitamins and minerals are deficient in a significant portion of the human population. Therefore, supplementation is a viable nutritional approach, which helps to maintain health and well-being. The supplementation efficiency of a highly hydrophobic compound such as cholecalciferol ($\log P > 7$) depends predominantly on the formulation. To overcome difficulties associated with the evaluation of pharmacokinetics of cholecalciferol, a method based on the short time absorption data in the clinical study and physiologically based mathematical modeling is proposed. The method was used to compare pharmacokinetics of liposomal and oily formulations of vitamin D₃. The liposomal formulation was more effective in elevating calcidiol concentration in serum. The determined AUC value for liposomal vitamin D₃ formulation was four times bigger than that for the oily formulation.

Keywords: cholecalciferol; vitamin D₃; liposomes; pharmacokinetics; absorption rate



Citation: Żurek, G.; Przybyło, M.; Witkiewicz, W.; Langner, M. Novel Approach for the Approximation of Vitamin D₃ Pharmacokinetics from In Vivo Absorption Studies. *Pharmaceutics* **2023**, *15*, 783. <https://doi.org/10.3390/pharmaceutics15030783>

Academic Editor: Paolo Magni

Received: 23 December 2022

Revised: 16 February 2023

Accepted: 25 February 2023

Published: 27 February 2023



Copyright: © 2023 by the authors. Licensee MDPI, Basel, Switzerland. This article is an open access article distributed under the terms and conditions of the Creative Commons Attribution (CC BY) license (<https://creativecommons.org/licenses/by/4.0/>).

1. Introduction

Vitamins are important for maintaining human health and wellbeing. Some of them are available only from exogenous sources as exemplified by vitamin C or vitamin B₁₂. Since they are not produced endogenously, the determination of their pharmacokinetics is a straightforward task, at least from the methodological point of view [1,2]. The pharmacokinetic curve of vitamin C can be derived from a short time clinical study. [3,4]. Vitamin D₃ is different. It originates from two sources: skin and foodstuff. This and the long half-time (about 20 days) make the determination of its pharmacokinetics challenging [5]. The most direct approach is to use a radiolabeled compound [6]. Regardless of the method used, there are numerous logistic and methodological difficulties making large-scale clinical studies demanding. In the paper, we propose a new method for vitamin D₃ pharmacokinetic curve determination. It combines semi-physiological modeling and short time absorption data from clinical studies.

Vitamin D₃ is a compound, of which a deficiency can lead to numerous health risks [7]. Its importance for human organism functioning is demonstrated by the fact that the vitamin is required for the expression of over 700 genes [8,9]. Vitamin D₃ is also critical element of calcium homeostasis [10]. The altered lifestyle of modern man (little exposure to natural sunlight) and changes in nutritional habits has resulted in wide-spread vitamin D₃ deficiency [7]. Therefore, effective modes of supplementation are an important element of preventive medicine [11].

Vitamin D₃ (cholecalciferol) is a precursor for its physiologically active metabolites calcidiol and calcitriol. The hydrophobic character of vitamin D₃ and its metabolites requires complex absorption and redistribution mechanisms [2,12]. This is because hydrophobic

compounds can be transferred across aqueous spaces only when associated with other molecule(s), forming water-soluble aggregates. This is critical since the cholecalciferol absorption (intestine) or synthesis (skin) are located in distal places with respect to the location of the first and the second steps of its metabolic transformation into the active form (liver and kidney). The transfer of hydrophobic compounds between the two locations requires mechanisms relying on dedicated and/or nonspecific carriers in the form of proteins and/or lipoproteins. Given orally, the cholecalciferol absorption consists of the sequence of events facilitated by ill-defined aggregates dispersed in the aqueous phase of the gastrointestinal tract. Vitamin D₃ can reach the intestine wall only when it is in the aggregate capable to cross the mucus layer [12]. When vitamin D₃ reaches enterocytes, it is internalized and released into serum while associated with specific carrier proteins (VDBP) [13,14] or with lipoproteins [15,16]. Its subsequent enzymatic transformation in the liver and kidneys is possible only because of this distribution system. Transport of vitamin D₃ and its metabolites is controlled by proteins and/or lipoprotein mediators.

It can be assumed that vitamin D₃ internalization, redistribution, and subsequent transformation to calcidiol (25(OH)D₃), which is routinely used for diagnostic purposes [17], can be qualitatively divided into two phases: before and after the internalization by competent cells in the intestine. Events prior to internalization by enterocytes are characterized by low specificity, whereas subsequent biodistribution and metabolic transformations are facilitated by very specific intracellular and extracellular events [9]. Absorption in the intestine can be greatly modified by changing the vitamin D₃ formulation. [18,19]. This is because hydrophobic vitamin D₃ is not capable of reaching the surface of the enterocyte alone. Instead, the absorption of vitamin D₃ consists of a sequence of physicochemical and enzyme-assisted transformations taking place in the gastrointestinal tract [20]. Because water insoluble crystals of vitamin D₃ cannot be effectively absorbed, it is commonly given as an oil formulation [15,21,22]. This by itself does not ensure efficient absorption since dispersion of oil in the aqueous phase will form an unstable and heterogenous emulsion [23,24]. For example, the coalescence of oily suspension will affect the digestion processes [12,25]. To be internalized, droplets of oil with vitamin D₃ should reach the surface of the enterocytes [26,27]. This happens only when oily droplets can cross the mucus layer containing polymeric mesh formed by mucins. The mucus serves as a filter, preventing large particulates (>400 nm) from reaching enterocytes [28]. Vitamin D₃ can be absorbed only when dissolved in particulates which are able to pass the mucus layer. This is difficult to achieve using the oily suspension alone [28,29]. All that will result is the limited capacity of an oily formulation to facilitate the efficient absorption of vitamin D₃ [22,30]. Liposomes are convenient and biocompatible oral delivery vehicles [16,22]. They easily accommodate the hydrophobic vitamin D₃ within their lipid bilayer and their size can be tailor-made. In addition, the mechanical stability of liposome lipid bilayer ensures that the cargo is delivered to the intestine wall ready for absorption [31,32]. In addition, when exposed to conditions simulating stomach and intestine environments (pH, temperature, bile salts and enzymes), their topology remains unchanged for a sufficiently long time to ensure the effective absorption. The main obstacle for the application of liposomes in everyday products has been the limited scale of available production processes and the belief that they are inherently unstable [33]. Those difficulties have been resolved by the introduction of Liposhell[®] technology, which is capable of delivering large quantities (tones) of a homogenous suspension of stable liposomes encapsulating a wide variety of active ingredients, including proteins and nucleic acids. The absorption of vitamin D₃ in liposomes relies on their endocytosis and trans-endocytosis by enterocytes and possible M cells [6,34]. In addition, the stability of liposomes in the suspension enhances the internalization, regardless of the accompanying foodstuff. Table 1 shows characteristic properties of the two formulations of vitamin D₃.

Table 1. Properties of liposomal and oily vitamin D₃ formulations relevant for the absorption in the intestine [15,18,19,27,35–37].

	Liposome	Oil
The outcome of the homogenization in stomach	predictable	unpredictable
Stability of the dispersion with respect to droplet size	high	low
Uniformity of droplet population	high	low
Stable droplet size distribution during digestion	medium	low
Ability to cross the mucus barrier	high	limited

The liposome suspension produced using Liposhell[®] technology is characterized by well-defined population of liposomes, ensuring optimal conditions for their internalization. The Liposhell[®] technology is based on the formation of tightly packed, uniform with respect to size, lipid vesicles (liposomal gel). The design of the liposome-based delivery strategy assumes that vitamin D₃ is located in the hydrophobic core of the lipid bilayer. The stability of the liposome-vitamin D₃ system with the presence of lipid vesicles and albumins was evaluated previously using isothermal titration calorimetry [38]. Specifically, no significant thermal signal was observed when liposomes with vitamin D₃ were added to vitamin D₃-free liposomes or albumins, showing that vitamin D₃ does not equilibrate between liposomes and albumin, nor between liposomes. From the experiment, it has been concluded that, during digestion, vitamin D₃ remains in liposomes regardless of their fate in the gastrointestinal tract.

2. Materials and Methods

2.1. Materials

Soybean phosphatidylcholine (Phospholipon 90G) and vitamin D₃ (cholecalciferol) were purchased from Lipoid GmbH (Ludwigshafen, Germany) and DSM Nutritional Product Ltd. (Village Neuf, France), respectively. Chloroform and methanol were obtained from VWR (Radnor, PA, USA), whereas ethanol and NaOH were from Stanlab (Lublin, Poland). All solutions were prepared with commercially purified water (AquaEngineering, Warsaw, Poland).

2.2. Preparation of Liposomal Vitamin D₃ Formulation

Liposomal vitamin D₃ formulation was prepared as described in details elsewhere [36]. In short, liposomes were formed by mixing the organic phase with the aqueous phase (1:1 *w/w*). The organic phase contains propylene glycol, phospholipids (20% *w/w* in the final preparation), and vitamin D₃. Next, the viscous gel was extruded through the 100 nm polycarbonate filter (Nucleopore Corp., Pleasanton, CA, USA). The content of phosphatidylcholine was determined by the HPLC-ELSD method [3]. Finally, the lipid gel was diluted 200 times with the glycerol/water (1:1 *w/w*) mixture and supplemented with natural flavor (0.3 *w/w*) and pectin (2.45 *w/w*). Liposomal vitamin D₃ was prepared by Lipid Systems Sp. z o.o. (Wrocław, Poland) under conditions satisfying HACCP and GMP requirements.

2.3. Characterization of Liposomal Vitamin D Formulation

The size distribution of liposomes in the liposomal vitamin D₃ formulation was determined by the dynamic light scattering method with some modifications in the preparation of the measured samples due to the presence of pectin (Zetasizer Nano ZS, Malvern, UK). The quantity of vitamin D₃ was determined with RP-HPLC (Reversed-Phase High Liquid Chromatography) according to the method developed by Sazali et al. [39], with some modifications. The modular HPLC set composed of a pump (Azura P4.1S, KNAUER, Berlin, Germany), autosampler (Marathon Basic, Spark Holland, Emmen, The Netherlands), peltier column thermostat (Jetstram II Plus, Knaure, Berlin, Germany), and a UV-VIS detector

(Azura UVD 2.1L, KNAUER, Berlin, Germany) was used. The separation was achieved using: 4.6×250 mm; $5 \mu\text{m}$ particles, 100 \AA pore sizes, column (Eurospher 100-5 C18, KNAUER, Berlin, Germany). The freshly prepared mixture of methanol and water (98:2 *v/v*) as the isocratic mobile phase was pumped at a flow rate of 1 mL/min at $40 \text{ }^\circ\text{C}$. The injection volume was $20 \mu\text{L}$. Samples for the calibration curve were prepared at the concentration range of $0.6\text{--}9 \mu\text{g/g}$ of vitamin D_3 in ethanol. Samples of liposomal formulations were dissolved in ethanol at the 4/10 (*w/w*) ratio, mixed, centrifuged (2800 rpm for 10 min.), and filtered through $0.2 \mu\text{m}$ cellulose membrane before analysis [40].

2.4. Cryogenic Transmission Electron Microscopy (TEM) Imaging

Cryogenic Transmission Electron Microscopy (cryo-TEM) images were collected with a Tecnai F20 X TWIN microscope (FEI Company, Hillsboro, OR, USA) equipped with a field emission gun operating at an acceleration voltage of 200 kV. Images were recorded on the Gatan Rio 16 CMOS 4 k camera and processed with Gatan Microscopy Suite (GMS) software (Gatan Inc., Pleasanton, CA, USA). Specimen preparation was done by the vitrification of the aqueous solutions on grids with holey carbon film (Quantifoil R 2/2; Quantifoil Micro Tools GmbH, Großlobichau, Germany). Prior to use, the grids were treated for 15 s in oxygen plasma using a Femto plasma cleaner (Diener Electronic, Ebhausen, Germany). Cryo-samples were prepared by applying a droplet ($3 \mu\text{L}$) of the suspension to the grid, blotting with filter paper, and immediate freezing in liquid ethane using a fully automated blotting device Vitrobot Mark IV (Thermo Fisher Scientific, Waltham, MA, USA). The vitrified specimens were kept under liquid nitrogen prior the insertion into a cryo-TEMholder Gatan 626 (Gatan Inc., Pleasanton, CA, USA) and analyzed at $-178 \text{ }^\circ\text{C}$.

2.5. Clinical Studies and Quantification of Calcidol in Serum

The clinical experiment has been thoroughly described elsewhere [36]. In summary, the study was performed on 18 healthy volunteers (age 24–65) according to “the cross-over design”. Following a 12 h fasting, each volunteer was given 10,000 IU of vitamin D_3 , either in the liposomal or oily formulation. After 3 weeks, the experiment was repeated, but volunteers consumed the other vitamin D_3 formulation. The marketed product was used as the oily formulation. The quantity of vitamin D_3 in oily formulation was used as specified by the producer. Less than $50 \mu\text{L}$ of blood was drawn from a finger of each volunteer at eight-time points; the reference sample shortly before and 0.5, 1, 1.5, 2, 3, 4, and 5 h following the intake of vitamin D_3 . Blood samples of the volunteer were collected by qualified personnel, and the concentration of $25(\text{OH})\text{D}_3$ measured by Cambridge Diagnostics Sp. z o.o. (Poland). All procedures involving humans were approved by the Bioethical Commission at the Research and Development Centre at the Specialized Hospital in Wrocław, number: KB/07/2020. The vitamin D_3 absorption was evaluated based on the concentration of calcidiol in serum. Specifically, the initial quantity of $25(\text{OH})\text{D}_3$ (shortly before supplementation, A_0) was subtracted from its values at later time points, $A(t)$, and the obtained difference normalized to the initial value $[(A(t) - A_0)/A_0]$. Next, the tendency of $25(\text{OH})\text{D}_3$ change was approximated with the linear function using the last square fitting. A straight line was then used to estimate the calcidiol concentration in serum for the pharmacokinetic curve reconstruction.

2.6. The Reconstruction of Pharmacokinetic Curve for Calcidol

The absorption of vitamin D_3 is followed by its transfer to the liver, where it is metabolically transformed. The literature data show that the pharmacokinetic curve for calcidiol reaches a maximum at three days after supplementation with cholecalciferol. However, the steep rise of calcidiol concentration in serum shortly after supplementation indicates rapid absorption and enzymatic transformation of cholecalciferol to calcidiol in the liver. The shape of the pharmacokinetic curve during the first day after supplementation justifies the assumption that calcidiol can be evaluated even during the first few hours following supplementation. The advantage of such approach is the elimination of possible interferences

resulting from unpredictable and difficult to control volunteer behavior, when outside the medical facility (exposure to the sun and/or variation in diets). Consequently, during the reduced time of the experiment, the observed rise of calcidiol is affected exclusively by the absorption efficiency. This is because, after fasting, the supplement will pass the absorption zone in the intestine during the few hours following the supplementation [41].

When a single dose of vitamin D₃ is administered, its quantity in serum can be described by the following formula:

$$[D_3(t)] = -k \int_0^t [D_3(t)] dt \quad (1)$$

where $[D_3(t)]$ represents the concentration of vitamin D₃ in serum. The amount of vitamin D₃ absorbed in the intestine $[D_3(0)]$ and can be expressed by the empirical formula [29]:

$$[D_3(0)] = \int_0^{t_{transit}} J_{muc}(t) dt \quad (2)$$

where $t_{transit}$ stands for the time, when vitamin D₃ resides in the region of intestine where the absorption is taking place, and $J_{muc}(t)$ represents the flux of vitamin D₃ across mucus lining the intestine wall. Parameters which define the absorbed quantity— $t_{transit}$ and $J_{muc}(t)$ —depend on vitamin D₃ formulation. When formulation disperses uniformly in the stomach content, the transit time will increase. No such effect will be observed when the coalescence occurs [16]. The flux of vitamin D₃ across the mucus will depend predominantly on properties of particulates such as surface charge, propensity for enzymatic activity, ability to accommodate bile acids, and most importantly their size. The size of particulates is an important parameter since mucus can be penetrated only when it does not exceed 400–500 nm [26,28].

The quantity of 25(OH)D₃ in serum can be approximated by the following equation:

$$[25(OH)D_3(t)] = \int_0^t \{k[D_3(t)] - m[25(OH)D_3(t)]\} dt \quad (3)$$

$[D_3(t)]$ is a cholecalciferol concentration, $[25(OH)D_3(t)]$ stands for the concentration of calcidiol, and k and m are constants describing the synthesis (liver) and degradation (kidneys) of calcidiol. It has been assumed that the quantity of vitamin D₃ at $t = 0$ equals to the amount of vitamin D₃(0) absorbed. The dependence of a calcidiol concentrations on time follows the formula:

$$[25(OH)D_3(t)] = \frac{ck}{m} + \frac{ke^{-kt}}{m-k} + \alpha e^{-mt} \quad (4)$$

Except the $[D_3(0)]$ value, all other parameters are dependent on metabolic processes. To calculate those parameters, the experimental data from the literature [42] were normalized and the function (4) was optimized with respect to k and m , assuming that the initial calcidiol concentration $C(0) = 0$. In addition, we assumed that, for a single application, $c = 0$ since $\log_{t \rightarrow \infty} C(t) = 0$. The optimization of the dissipation function equals the average distance between experimental and theoretical points. Consequently, the pharmacokinetic curve of calcidiol can be reconstructed from the combination of time-limited clinical studies and mathematical equations derived from experimental data [42].

3. Results and Discussion

The absorption of vitamin D₃ in liposomes is most efficient when their size does not exceed 250–300 nm [43]. Figure 1 shows the size distribution of liposomes along with the respective correlation function determined using dynamic light scattering. The average size of liposomes and polydispersity index (PDI) were equal to 117 nm. and 0.23, respectively. Visualization of liposomes with cryoTEM demonstrated that they are spherical, unilamellar, and confirmed the homogeneity of their size distribution. When an oily formulation of

vitamin D₃ is dispersed in water, it forms a heterogenous emulsion. The two formulations are expected to behave differently in the gastrointestinal tract, affecting the absorption efficiency of vitamin D₃. The short clinical experiment showed that the measured absorption rate, evaluated with slopes of linear functions, were statistically different and equaled to $7.03 \times 10^{-5} \text{ 1/min} \pm 3.02 \times 10^{-4} \text{ 1/min}$ and $4.01 \times 10^{-4} \text{ 1/min} \pm 7.12 \times 10^{-4} \text{ 1/min}$ for oily and liposomal formulations, respectively [35]. Those values were used to calculate the calcidiol concentration in serum at $t_{transit}$. The developed method was next used in studies regarding characterization of two vitamin D₃ formulations. In the analysis it had been assumed that the quantity of cholecalciferol and calcidiol in serum were at a concentration range where all proteins involved in cholecalciferol absorption, distribution, and metabolic transformation were not saturated. This means that the quantities of the absorbed cholecalciferol and the concentration of calcidiol in serum can be quantitatively correlated. Examples of pharmacokinetic curves derived for persons with vitamin D₃ deficiency for two different formulations (oily and liposomal) are presented on Figure 2.

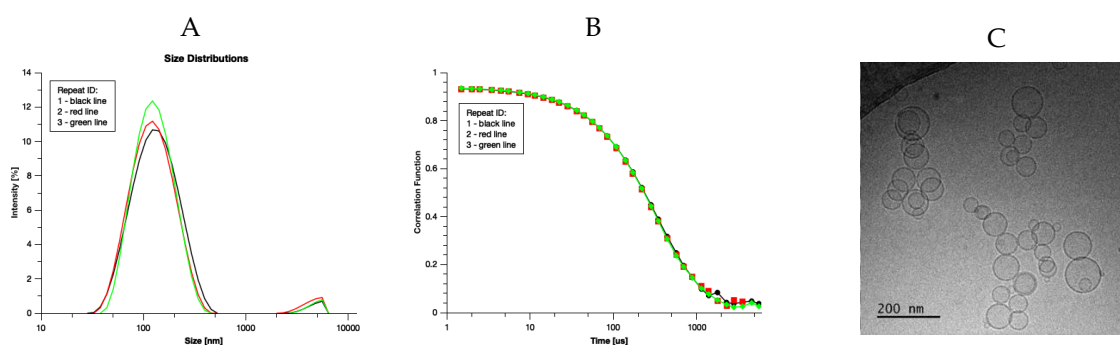


Figure 1. Size distribution of liposomes with vitamin D₃. Panel (A) shows the liposome size distributions. Panel (B) presents correlation functions. The average diameter of liposomes and polydispersity index were equal to 117 nm and 0.23, respectively. Panel (C) presents the cryoTEM image of liposomes with vitamin D₃.

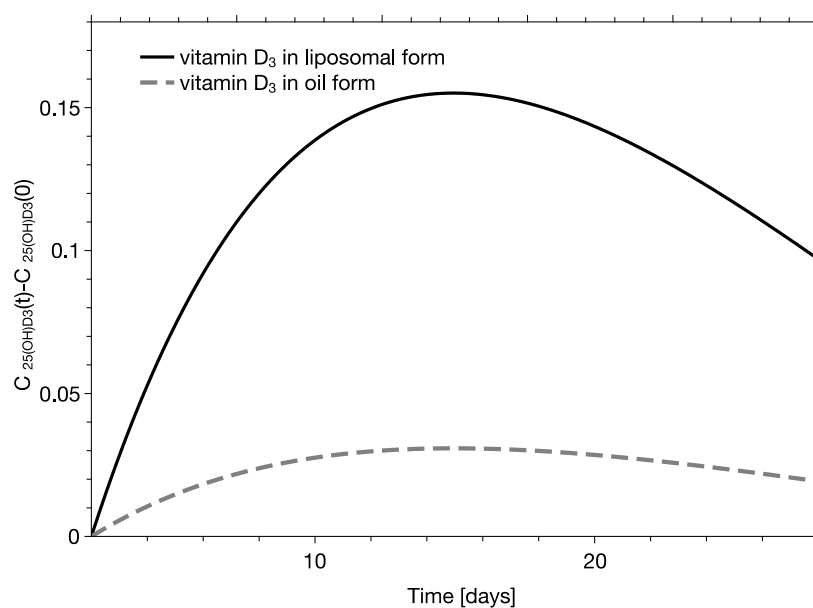


Figure 2. Example of the dependence of the increase of calcidiol concentration in serum ($C_{25(OH)D_3}(t) - C_{25(OH)D_3}(0)$) on time, as determined for a randomly selected person characterized by a low initial calcidiol concentration. The continuous and dotted curves represent the liposomal and oily formulation, respectively. The concentration of calcidiol in serum is in ng/L.

The reconstructed pharmacokinetic profiles of the oily and liposomal formulations were assessed using the standard single-compartmental pharmacokinetic analysis. Using the methodology, the following pharmacokinetic parameters have been derived: the maximum concentration of calcidiol (C_{\max}), the area under curve for the first day following the dose ($AUC_{1\text{day}}$), the area under the curve calculated from the 2nd to the 30th day following the dose ($AUC_{2\text{day-30days}}$), and the $AUC_{1\text{day-30day}}$ —the area under the plasma concentration–time curve integrated from zero to 30 days following the supplementation ($AUC_{1\text{day-30day}}$), calculated as a sum of $AUC_{1\text{day}}$ and $AUC_{2\text{day-30day}}$. The time at which the maximum concentration is reached (T_{\max}) and the elimination half-life of calcidiol ($t_{1/2}$) depend exclusively on metabolic processes, meaning that they do not depend on the type of formulation [42] (Table 2).

Table 2. Examples of quantitative values of pharmacokinetic parameters determined for a person with significant vitamin D₃ deficiency.

Parameter	Liposome Formulation	Oil Formulation
C_{\max}	0.335 [ng/L]	0.067 [ng/L]
T_{\max}	14 days	14 days
$t_{1/2}$	43 days	43 days
$AUC_{1\text{day}}$	0.135 [day·ng/L]	0.027 [day·ng/L]
$AUC_{2\text{days-30day}}$	8.646 [day·ng/L]	1.718 [day·ng/L]
$AUC_{1\text{day-30day}}$	8.511 [day·ng/L]	1.692 [day·ng/L]

The pharmacokinetics of calcidiol following the supplementation with cholecalciferol depends on the vitamin D₃ formulation. Clinical experiment has shown that for persons with a significant deficiency of vitamin D₃, the application of liposomal formulation causes a significant and rapid increase of calcidiol concentration in serum. The effect of the oily formulation of cholecalciferol is much smaller. Specifically, $AUC_{1\text{day}}$ determined for calcidiol, reflecting the efficiency of cholecalciferol absorption, increased from 0.037 [day·ng/L] to 0.135 [day·ng/L], almost 3.6 times, which makes the increase of the $AUC_{1\text{day-30day}}$ from 1.69 [day·ng/L] to 8.5 [day·ng/L], i.e., 5 times. The $AUC_{1\text{day-30day}}$ relates to pharmacokinetics of calcidiol, which depends on the quantity of absorbed cholecalciferol and physiological processes affecting its serum concentration. The increase in the maximum concentration of calcidiol is also substantially elevated from 0.067 [day·ng/L] to 0.335 [day·ng/L]. Derived numbers confirmed the prediction that liposomes with well-defined sizes are a far more effective formulation in delivering hydrophobic vitamin D₃ than their oily equivalent.

4. Discussion

The vitamin D₃ digestion and absorption processes depend on physiological factors such as low pH and mechanical agitation in the stomach, followed by enzymatic degradation and bile acid emulsification in the intestine. In addition, the digestion will be affected by the presence of foodstuffs and the type of vitamin D₃ formulation [12]. The two formulations of cholecalciferol (oil and liposomes) selected for comparison are qualitatively different. Since the formation of an emulsion from the oily formulation is taking place in the gastrointestinal tract, it is impossible to control, and the resulting dispersion of oil will be heterogenous with propensity to coalesce [26,29]. The suspension of liposomes is different; it is a two-phase system, where the hydrophobic region of the spherical lipid bilayer separates two aqueous phases. Liposomes can be produced in such a way that they will form a suspension, which is uniform with respect to the liposome size. In such a system, cholecalciferol is in the hydrophobic region of a liposome-forming lipid bilayer [36]. Liposomes are very stable structures, which cannot be easily destabilized unless their chemical composition is altered. This can be achieved by the action of digestive enzymes or by an association with natural detergents (bile acids) [31,32]. Importantly, dilution or

mixing of liposome suspension with foodstuff will not affect their topology, nor their size. The uniform distribution of liposomes within foodstuff results in the extended exposure time. In addition, with appropriate sizes (less than 400 nm), liposomes can enter body compartments by two independent pathways: endocytotic and transendocytotic. Whereas the pathway from endosome to chylomicrons is complicated and time-consuming [44], transcytosis will result in intact liposomes crossing the intestine wall and rapidly entering the immunological system [27]. The latter will accelerate the appearance of cholecalciferol in serum and the subsequent transformation to calcidiol.

The oily formulation behaves differently; it may coalesce in the stomach, shortening the exposure time to enterocytes. The additional factor affecting the absorption of vitamin D₃ from the oily formulation is its high heterogeneity and low stability upon digestion. In summary, whereas liposomes will remain unchanged or decrease in size, the sizes of oily droplets, characterized by their propensity to coalesce, will increase [35]. With the much shorter residence time in the intestine and a non-optimal size distribution, only a fraction of oil (vitamin D₃) will have access to the surface of enterocytes. The vitamin D₃ redistribution mechanisms and its transformation to calcidiol in the liver make it difficult to alter metabolic processes. Consequently, it can be assumed that the quantity of calcidiol will scale with the amount of absorbed vitamin D₃. The quantity of absorbed vitamin D₃ from a dose will depend on the exposure time and formulation-dependent accessibility for competent cells. The exposure time is a function of peristaltic activity, stomach content, and the distribution of vitamin D₃. Clinical data presented by Armas et al. [42] shows the pharmacokinetics of radiolabeled vitamin D₂ and vitamin D₃ following oral administration. The dependence of concentration profiles in the absorption phase of the two formulations are very similar. Dependence of the concentration of calcidiol as a function of time is different. The maximum is reached only on the 5th day for vitamin D₂ and on about the 15th day for vitamin D₃. These data show that the absorption and biodistribution processes can be analyzed separately and that the character of calcidiol pharmacokinetic curves will be affected by the quantity of absorbed vitamins and the efficiency of the subsequent metabolic processes. Rapid absorption of vitamin D₃ justifies the approach, in which the initial rise of calcidiol serum concentration is driven predominantly by the quantity of absorbed vitamin D₃. Later, when the absorption phase is completed, the pharmacokinetic profile of calciferol depends exclusively on the metabolic processes [8]. Therefore, the shape of the pharmacokinetic curve is preserved, but the value of AUC will depend exclusively on the quantity of the absorbed vitamin [12,20,45–47]). Consequently, the pharmacokinetic curve for a formulation can be reconstructed from the quantity of absorbed vitamin D₃ and the predetermined shape of the pharmacokinetic curve [1,48,49].

5. Conclusions

The effective supplementation of hydrophobic vitamin D₃ requires the application of excipients, which will facilitate its dissolution. However, this by itself will not ensure its effective absorption. The efficient vitamin D₃ absorption will take place from formulations in the form of droplets characterized by sizes smaller than 250–300 nm, resulting from the size of the intestine mucus pores [43]. Dispersion of liposomes with vitamin D₃ is an example of such a formulation. The absorption of vitamin D₃ in liposomal and oily formulations was evaluated using short-term absorption data supplemented with physiology-based mathematical modeling. The quantity of absorbed vitamin D₃ in vivo was estimated with the increased concentration of calcidiol in serum, whereas the shape of the pharmacokinetic curve was reconstructed with a physiologically based mathematical model. The analysis shows that the liposomal vitamin D₃ formulation is more effective than its oily solution.

Author Contributions: Conceptualization, M.L. and M.P.; methodology, M.L.; software, G.Ż.; validation, M.L. and M.P., formal analysis, G.Ż.; investigation, M.L.; resources, M.P.; data curation, G.Ż.; writing—original draft preparation, M.L.; writing—review and editing, M.P. and W.W.; visualization, G.Ż. and M.P.; supervision, M.L. and W.W.; project administration, M.L.; funding acquisition, M.P. All authors have read and agreed to the published version of the manuscript.

Funding: This work was supported by the National Centre for Research and Development under grant number POIR.04.01.04-00-0159/17-00.

Institutional Review Board Statement: Not applicable.

Informed Consent Statement: Not applicable.

Data Availability Statement: Not applicable.

Acknowledgments: CryoTEM images have been provided by Barbara Trzebicka and Aleksander Foryś, from the Centre of Polymer and Carbon Materials, Polish Academy of Sciences, Zabrze, Poland.

Conflicts of Interest: M.P. and M.L. are partners in Lipid Systems sp. z o.o.

References

1. Ramakrishnan, V.; Yang, Q.J.; Quach, H.; Cao, Y.; Chow, E.; Mager, D.; Pang, S. Physiologically-Based Pharmacokinetic-Pharmacodynamic Modeling of 1 alpha,25-Dihydroxyvitamin D-3 in Mice. *Drug Metab. Dispos.* **2016**, *44*, 189–208. [[CrossRef](#)] [[PubMed](#)]
2. Sawyer, M.E.; Tran, H.T.; Evans, M.V. A physiologically based pharmacokinetic model of vitamin D. *J. Appl. Toxicol.* **2017**, *37*, 1448–1454. [[CrossRef](#)] [[PubMed](#)]
3. Łukawski, M.; Dałek, P.; Borowik, T.; Foryś, A.; Langner, M.; Witkiewicz, W.; Przybyło, M. New oral liposomal vitamin C formulation: Properties and bioavailability. *J. Liposome Res.* **2019**, *30*, 227–234. [[CrossRef](#)] [[PubMed](#)]
4. Padayatty, S.J.; Sun, H.; Wang, Y.; Riordan, H.D.; Hewitt, S.M.; Katz, A.; Wesley, R.A.; Levine, M. Vitamin C Pharmacokinetics: Implications for Oral and Intravenous Use. *Ann. Intern. Med.* **2004**, *140*, 533–537. [[CrossRef](#)] [[PubMed](#)]
5. Gil, Á.; Plaza-Diaz, J.; Mesa, M.D. Vitamin D: Classic and Novel Actions. *Ann. Nutr. Metab.* **2018**, *72*, 87–95. [[CrossRef](#)] [[PubMed](#)]
6. Shane, B. Folate and vitamin B12 metabolism: Overview and interaction with riboflavin, vitamin B6, and polymorphisms. *Food Nutr. Bull.* **2008**, *29* (Suppl. S2), S5–S16; discussion S17–S19. [[CrossRef](#)]
7. Wilson, L.; Tripkovic, L.; Hart, K.; Lanham-New, S. Vitamin D deficiency as a public health issue: Using vitamin D-2 or vitamin D-3 in future fortification strategies. *Proc. Nutr. Soc.* **2017**, *76*, 392–399. [[CrossRef](#)]
8. Pilz, S.; Zittermann, A.; Trummer, C.; Theiler-Schwetz, V.; Lerchbaum, E.; Keppel, M.H.; Grübler, M.R.; März, W.; Pandis, M. Vitamin D testing and treatment: A narrative review of current evidence. *Endocr. Connect.* **2019**, *8*, R27–R43. [[CrossRef](#)]
9. Carlberg, C. Nutrigenomics of Vitamin D. *Nutrients* **2019**, *11*, 676. [[CrossRef](#)]
10. Anderson, P.H. Vitamin D Activity and Metabolism in Bone. *Curr. Osteoporos. Rep.* **2017**, *15*, 443–449. [[CrossRef](#)]
11. Moulas, A.N.; Vaiou, M. Vitamin D fortification of foods and prospective health outcomes. *J. Biotechnol.* **2018**, *285*, 91–101. [[CrossRef](#)] [[PubMed](#)]
12. Maurya, V.K.; Aggarwal, M. Factors influencing the absorption of vitamin D in GIT: An overview. *J. Food Sci. Technol.* **2017**, *54*, 3753–3765. [[CrossRef](#)] [[PubMed](#)]
13. Denburg, M.R.; Bhan, I. Vitamin D-Binding Protein in Health and Chronic Kidney Disease. *Semin. Dial.* **2015**, *28*, 636–644. [[CrossRef](#)] [[PubMed](#)]
14. Jorde, R. The Role of Vitamin D Binding Protein, Total and Free 25-Hydroxyvitamin D in Diabetes. *Front. Endocrinol.* **2019**, *10*, 79. [[CrossRef](#)] [[PubMed](#)]
15. Gupta, R.; Behera, C.; Paudwal, G.; Rawat, N.; Baldi, A.; Gupta, P.N. Recent Advances in Formulation Strategies for Efficient Delivery of Vitamin D. *AAPS PharmSciTech* **2018**, *20*, 11. [[CrossRef](#)]
16. Rezhdo, O.; Speciner, L.; Carrier, R. Lipid-associated oral delivery: Mechanisms and analysis of oral absorption enhancement. *J. Control. Release* **2016**, *240*, 544–560. [[CrossRef](#)] [[PubMed](#)]
17. Herrmann, M.; Farrell, C.-J.L.; Pusceddu, I.; Fabregat-Cabello, N.; Cavalier, E. Assessment of vitamin D status—A changing landscape. *Clin. Chem. Lab. Med.* **2017**, *55*, 3–26. [[CrossRef](#)]
18. Corstens, M.N.; Berton-Carabin, C.; De Vries, R.; Troost, F.J.; Masclee, A.A.M.; Schroen, K. Food-grade micro-encapsulation systems that may induce satiety via delayed lipolysis: A review. *Crit. Rev. Food Sci. Nutr.* **2015**, *57*, 2218–2244. [[CrossRef](#)]
19. Guo, Q.; Bellissimo, N.; Rousseau, D. The Physical State of Emulsified Edible Oil Modulates Its in Vitro Digestion. *J. Agric. Food Chem.* **2017**, *65*, 9120–9127. [[CrossRef](#)]
20. Borel, P.; Caillaud, D.; Cano, N.J. Vitamin D Bioavailability: State of the Art. *Crit. Rev. Food Sci. Nutr.* **2015**, *55*, 1193–1205. [[CrossRef](#)]

21. Hayes, A.; Cashman, K.D. Food-based solutions for vitamin D deficiency: Putting policy into practice and the key role for research. *Proc. Nutr. Soc.* **2016**, *76*, 54–63. [[CrossRef](#)] [[PubMed](#)]
22. Hsu, C.-Y.; Wang, P.-W.; Alalaiwe, A.; Lin, Z.-C.; Fang, J.-Y. Use of Lipid Nanocarriers to Improve Oral Delivery of Vitamins. *Nutrients* **2019**, *11*, 68. [[CrossRef](#)] [[PubMed](#)]
23. Mao, L.; Wang, D.; Liu, F.; Gao, Y. Emulsion design for the delivery of beta-carotene in complex food systems. *Crit. Rev. Food Sci. Nutr.* **2018**, *58*, 770–784. [[CrossRef](#)] [[PubMed](#)]
24. Ozturk, B.; Argin, S.; Ozilgen, M.; McClements, D.J. Nanoemulsion delivery systems for oil-soluble vitamins: Influence of carrier oil type on lipid digestion and vitamin D3 bioaccessibility. *Food Chem.* **2015**, *187*, 499–506. [[CrossRef](#)] [[PubMed](#)]
25. Borel, P.; Desmarchelier, C. Bioavailability of Fat-Soluble Vitamins and Phytochemicals in Humans: Effects of Genetic Variation. *Annu. Rev. Nutr.* **2018**, *38*, 69–96. [[CrossRef](#)]
26. Ensign, L.M.; Cone, R.; Hanes, J. Oral drug delivery with polymeric nanoparticles: The gastrointestinal mucus barriers. *Adv. Drug Deliv. Rev.* **2012**, *64*, 557–570. [[CrossRef](#)] [[PubMed](#)]
27. Xia, F.; Fan, W.; Jiang, S.; Ma, Y.; Lu, Y.; Qi, J.; Ahmad, E.; Dong, X.; Zhao, W.; Wu, W. Size-Dependent Translocation of Nanoemulsions via Oral Delivery. *ACS Appl. Mater. Interfaces* **2017**, *9*, 21660–21672. [[CrossRef](#)]
28. Cone, R.A. Barrier properties of mucus. *Adv. Drug Deliv. Rev.* **2009**, *61*, 75–85. [[CrossRef](#)]
29. Bornhorst, G.M.; Gouseti, O.; Wickham, M.S.; Bakalis, S. Engineering Digestion: Multiscale Processes of Food Digestion. *J. Food Sci.* **2016**, *81*, R534–R543. [[CrossRef](#)]
30. Porter, C.; Pouton, C.; Cuine, J.; Charman, W. Enhancing intestinal drug solubilization using lipid-based delivery systems. *Adv. Drug Deliv. Rev.* **2008**, *60*, 673–691. [[CrossRef](#)]
31. Doskocz, J.; Dałek, P.; Foryś, A.; Trzebicka, B.; Przybyło, M.; Mesarec, L.; Iglič, A.; Langner, M. The effect of lipid phase on liposome stability upon exposure to the mechanical stress. *Biochim. Biophys. Acta-Biomembr.* **2020**, *1862*, 183361. [[CrossRef](#)] [[PubMed](#)]
32. Doskocz, J.; Dałek, P.; Przybyło, M.; Trzebicka, B.; Foryś, A.; Kobylukh, A.; Iglič, A.; Langner, M. The Elucidation of the Molecular Mechanism of the Extrusion Process. *Materials* **2021**, *14*, 4278. [[CrossRef](#)] [[PubMed](#)]
33. Wu, W.; Lu, Y.; Qi, J. Oral delivery of liposomes. *Ther. Deliv.* **2015**, *6*, 1239–1241. [[CrossRef](#)] [[PubMed](#)]
34. Zhang, J.; Chang, D.; Yang, Y.; Zhang, X.; Tao, W.; Jiang, L.; Liang, X.; Tsai, H.; Huang, L.; Mei, L. Systematic investigation on the intracellular trafficking network of polymeric nanoparticles. *Nanoscale* **2017**, *9*, 3269–3282. [[CrossRef](#)]
35. Raikos, V.; Ranawana, V. Designing emulsion droplets of foods and beverages to enhance delivery of lipophilic bioactive components—A review of recent advances. *Int. J. Food Sci. Technol.* **2016**, *52*, 68–80. [[CrossRef](#)]
36. Dałek, P.; Drabik, D.; Wolczańska, H.; Foryś, A.; Jagas, M.; Jędruchiewicz, N.; Przybyło, M.; Witkiewicz, W.; Langner, M. Bioavailability by design—Vitamin D3 liposomal delivery vehicles. *Nanomed. Nanotechnol. Biol. Med.* **2022**, *43*, 102552. [[CrossRef](#)] [[PubMed](#)]
37. Nowak, J.K.; Sobkowiak, P.; Drzymała-Czyż, S.; Krzyżanowska-Jankowska, P.; Sapiejka, E.; Skorupa, W.; Pogorzelski, A.; Nowicka, A.; Wojsyk-Banaszak, I.; Kurek, S.; et al. Fat-Soluble Vitamin Supplementation Using Liposomes, Cyclodextrins, or Medium-Chain Triglycerides in Cystic Fibrosis: A Randomized Controlled Trial. *Nutrients* **2021**, *13*, 4554. [[CrossRef](#)]
38. Fanali, G.; di Masi, A.; Trezza, V.; Marino, M.; Fasano, M.; Ascenzi, P. Human serum albumin: From bench to bedside. *Mol. Asp. Med.* **2012**, *33*, 209–290. [[CrossRef](#)]
39. Sazali, N.H.; Alshishani, A.; Saad, B.; Chew, K.Y.; Chong, M.M.; Miskam, M. Salting-out assisted liquid–liquid extraction coupled with high-performance liquid chromatography for the determination of vitamin D3 in milk samples. *R. Soc. Open Sci.* **2019**, *6*, 190952. [[CrossRef](#)]
40. Ibarguren, M.; Alonso, A.; Tenchov, B.G.; Goñi, F.M. Quantitation of cholesterol incorporation into extruded lipid bilayers. *Biochim. Biophys. Acta-Biomembr.* **2010**, *1798*, 1735–1738. [[CrossRef](#)]
41. Jamei, M.; Turner, D.; Yang, J.; Neuheff, S.; Polak, S.; Rostami-Hodjegan, A.; Tucker, G. Population-Based Mechanistic Prediction of Oral Drug Absorption. *AAPS J.* **2009**, *11*, 225–237. [[CrossRef](#)] [[PubMed](#)]
42. Armas, L.A.G.; Hollis, B.W.; Heaney, R.P. Vitamin D2 is much less effective than vitamin D3 in humans. *J. Clin. Endocrinol. Metab.* **2004**, *89*, 5387–5391. [[CrossRef](#)] [[PubMed](#)]
43. Carlson, T.L.; Lock, J.Y.; Carrier, R.L. Engineering the Mucus Barrier. *Annu. Rev. Biomed. Eng.* **2018**, *20*, 197–220. [[CrossRef](#)] [[PubMed](#)]
44. Julve, J.; Martín-Campos, J.M.; Escolà-Gil, J.C.; Blanco-Vaca, F. Chylomicrons: Advances in biology, pathology, laboratory testing, and therapeutics. *Clin. Chim. Acta* **2016**, *455*, 134–148. [[CrossRef](#)] [[PubMed](#)]
45. Chun, R.F.; Peercy, B.E.; Orwoll, E.S.; Nielson, C.M.; Adams, J.S.; Hewison, M. Vitamin D and DBP: The free hormone hypothesis revisited. *J. Steroid Biochem. Mol. Biol.* **2013**, *144*, 132–137. [[CrossRef](#)]
46. Kuai, R.; Li, D.; Chen, Y.E.; Moon, J.J.; Schwendeman, A. High-Density Lipoproteins: Nature’s Multifunctional Nanoparticles. *ACS Nano* **2016**, *10*, 3015–3041. [[CrossRef](#)]
47. Silva, M.C.; Furlanetto, T.W. Intestinal absorption of vitamin D: A systematic review. *Nutr. Rev.* **2017**, *76*, 60–76. [[CrossRef](#)]

48. Ocampo-Pelland, A.S.; Gastonguay, M.R.; French, J.F.; Riggs, M. Model-based meta-analysis for development of a population-pharmacokinetic (PPK) model for Vitamin D3 and its 25OHD3 metabolite using both individual and arm-level data. *J. Pharmacokinet. Pharmacodyn.* **2016**, *43*, 191–206. [[CrossRef](#)]
49. Ocampo-Pelland, A.S.; Gastonguay, M.R.; Riggs, M. Model-based meta-analysis for comparing Vitamin D2 and D3 parent-metabolite pharmacokinetics. *J. Pharmacokinet. Pharmacodyn.* **2017**, *44*, 375–388. [[CrossRef](#)]

Disclaimer/Publisher’s Note: The statements, opinions and data contained in all publications are solely those of the individual author(s) and contributor(s) and not of MDPI and/or the editor(s). MDPI and/or the editor(s) disclaim responsibility for any injury to people or property resulting from any ideas, methods, instructions or products referred to in the content.